PHYSICAL REVIEW E **91**, 062141 (2015)

Nonuniversal surface behavior of dynamic phase transitions

Patricia Riego and Andreas Berger
CIC nanoGUNE, E-20018 Donostia-San Sebastian, Spain

(Received 27 April 2015; published 29 June 2015)

We have studied the dynamic phase transition (DPT) of the kinetic Ising model in systems with surfaces within the mean-field approximation. Varying the surface exchange coupling strength J_s, the amplitude of the externally applied oscillating field h_0, and its period P, we explore the dynamic behavior of the layer-dependent magnetization and the associated DPTs. The surface phase diagram shows several features that resemble those of the equilibrium case, with an extraordinary bulk transition and a surface transition for high J_s values, independent from the value of h_0. For low J_s, however, h_0 is found to be a crucial parameter that leads to nonuniversal surface behavior at the ordinary bulk transition point. Specifically, we observed here a bulk-supported surface DPT for high field amplitudes h_0 and correspondingly short critical periods P_c, whereas this surface transition simultaneous to the bulk one is suppressed for slow critical dynamics occurring for low values of h_0. The suppression of the DPT for low h_0 not only occurs for the topmost surface layer, but also affects a significant number of subsurface layers. We find that the key physical quantity that explains this nonuniversal behavior is the time correlation between the dynamic surface and bulk magnetizations at the bulk critical point. This time correlation has to pass a threshold value to trigger a bulk-induced DPT in the surface layers. Otherwise, dynamic phase transitions are absent at the surface in stark contrast to the equilibrium behavior of the corresponding thermodynamic Ising model. Also, we have analyzed the penetration depth of the dynamically ordered phase for the surface DPT that occurs for large J_s values. Here we find that the penetration depth depends strongly on J_s and behaves identically to the corresponding equilibrium Ising model.

DOI: 10.1103/PhysRevE.91.062141 PACS number(s): 64.60.Ht, 68.35.Rh, 05.70.Ln, 75.10.Hk

I. INTRODUCTION

Magnetic systems in the ferromagnetic phase, i.e., below the Curie temperature T_c, have been found to exhibit a dynamic phase and a related nonequilibrium dynamic phase transition (DPT) when driven by an external periodically oscillating field [1]. This occurs when the period P of the applied oscillating field becomes comparable to the relaxation time τ of the magnetic or spin system. In this case, the time-dependent magnetization is unable to reverse before the sign of the magnetic field changes again and the system is in a dynamically ordered phase. This phenomenon was first studied by Tomé and Oliveira [1], who analyzed the kinetic Ising model within the mean-field approximation (MFA).

Subsequent studies using different methodologies such as the MFA and Monte Carlo simulations (MCSs) [2–5] focused on the question of how the shape and area of hysteresis loops depend on the period and amplitude of the magnetic field. For large periods, the area of the hysteresis loop follows a scaling behavior, while the center of the hysteresis loop deviates from zero if the field changes are fast, i.e., when the oscillation period P is sufficiently small. This type of behavior has also been confirmed experimentally in ultrathin films [6,7]. Further theoretical investigations of the kinetic Ising model [8–23] have analyzed various aspects of the DPT and concluded that the period-averaged magnetization Q plays the role of the dynamic order parameter, showing a nonzero value in the dynamically ordered phase, when the period of the oscillating field is below a certain critical period P_c, while being zero above P_c in the dynamically disordered phase. It has also been shown that the DPT occurs at a critical point P_c and that there is a power law for Q in the vicinity of P_c that exhibits the same critical exponent as in the thermodynamic equilibrium case. Hence, it is well established that the kinetic Ising model for a bulk system belongs to the same universality class as the corresponding equilibrium model. The question of the existence of a conjugate field of Q, analogous to the external magnetic field being the conjugate field of the magnetization in the thermodynamic case, has been addressed relatively recently [16,20,22,24]. These studies point out that this role is played by an external continuous bias field h_b that is applied in addition to the periodic oscillatory field that drives the DPT in the first place. The equation of state for the kinetic Ising model within the MFA was derived [22], verifying this role of h_b, at least within the mean-field approximation. Some experimental works on the DPT have gone beyond a mere observation of the collapse of the hysteresis loop area with decreasing field period and instead enabled a quantitative study of the dynamic order parameter Q as a function of P and h_b [25,26].

All these previously mentioned theoretical works have studied the DPT without the explicit consideration of surfaces. However, the presence of surfaces is known to have a substantial impact on local quantities at bulk critical points in equilibrium. For the thermodynamic case, this fact has been subject to extensive studies [27–35] and it is well understood. Depending on the exchange coupling strength between neighboring spins within the surface J_s compared to that between spins in the bulk J_b, two regimes are observed. For low J_s values, the surface, which would not undergo a phase transition by itself at the bulk critical point T_c, is polarized by the bulk. Consequently, both the surface and bulk undergo a phase transition at the bulk T_c in unison. As the surface is already ordered through the support of the bulk, it does not show its own phase transition, which would otherwise occur at a lower temperature. This regime is called the ordinary transition. Even if both the surface and bulk order at the same T_c in this low J_s case, their critical exponents differ. Within the MFA one obtains, for instance, $\beta_b = 1/2$ for the bulk and

$\beta_s = 1$ for the surface. If the surface exchange coupling is sufficiently enhanced over its bulk value, however, the surface can order separately at higher temperatures than the bulk, which is the so-called surface transition. For such systems, the bulk undergoes the so-called extraordinary transition at its own T_c in the presence of an already ordered surface. In this case, the surface ordering is two dimensional, whereas the bulk one is three dimensional.

The nonequilibrium properties of a system with surfaces under the effect of an external oscillating field, however, are not yet fully understood. Only very recently, several authors have studied the DPT in systems with surfaces [36–43] to shed light on this subject. Hereby, some intriguing observations have been made. For instance, surface critical exponents in the DPT were found to differ from the values of the equilibrium surface critical exponents [36], thus indicating that the dynamic surface universality class is different from that of the equilibrium surface system. This is in strong contrast with what one observes for the bulk system, where both kinetic and equilibrium Ising models exhibit the same critical exponents. Furthermore, it was reported that the kinetic surface phase diagram resembles the equilibrium one, characterized by a distinct surface transition and an extraordinary bulk transition for high values of J_s and an ordinary bulk transition for low values of J_s. However, the pioneering work of Tauscher and Pleimling [40] has revealed the fact that for sufficiently weak surface couplings, the surface does not undergo a DPT triggered by the bulk, in distinct contrast to the behavior of the equilibrium Ising model, where the surface follows the bulk transition no matter how low J_s is.

The main purpose of our work is to perform a broad-based investigation of the DPT in systems with surfaces. To enable a wide parameter space exploration, we have realized our calculations by utilizing the mean-field methodology because it is computationally far less demanding. In particular, this approach has enabled us to investigate the role that the oscillating field amplitude h_0 plays. We have concluded that h_0 is a very relevant parameter that determines not only the exact location of the phase transition point P_c, but also the actual presence or absence of the DPT at the surface when the value of J_s is low. Thus, we find that the occurrence of the DPT at surfaces is not a universal behavior or phenomenon, but instead dependent on the specific external parameter set that determines the location of the bulk DPT. We have also explored the underlying physical mechanism that is responsible for this lack of universal behavior. For this purpose, we have analyzed the time correlation between the time-dependent surface and bulk magnetizations and we have identified this correlation as the relevant physical parameter that triggers a bulk-supported surface DPT. In addition to the analysis of the topmost surface layer, we also performed a layer-dependent analysis, enabling us to identify relevant quantities as a function of depth. In particular, we observe not only that the DPT is suppressed at the topmost surface layer for certain low J_s and low h_0 cases, but that there are approximately five subsurface layers that are not participating in the bulk-triggered DPT at P_c either. For the high J_s cases, the layer resolution enables us to study the penetration of the localized surface transition into the layers below the surface, which happens at critical periods above the bulk P_c.

The paper is organized as follows. In Sec. II we explain the method that we have applied to perform the mean-field calculations. In Sec. III we discuss the results for two particular cases: in Sec. III A for the bulk-terminated case ($J_s = J_b$) and in Sec. III B for a modified surface coupling strength with respect to that of the bulk ($J_s \neq J_b$). Finally, in Sec. IV we summarize our study, relate it to prior work, and discuss its implications for future theoretical and experimental work.

II. METHOD

In our calculations we apply the MFA to explore the DPT in systems with surfaces. For the sake of comparability with previous theoretical studies [40,41], the system under study is chosen to be a simple cubic lattice with (100) surface orientation [44], which is depicted schematically in Fig. 1. A series of atoms organized in layers from $L = 1$ to $L = N$ is coupled with an exchange coupling strength J_s, for nearest-neighbor spin pairs in $L = 1$, and with J_b, for nearest-neighbor spin pairs in which at least one spin is not located in $L = 1$. The Ising Hamiltonian that describes this spin system, normalized to J_b, is given by

$$\tilde{\mathcal{H}} = -\frac{J_s}{J_b}\sum_{[i,j]} S_i S_j - \sum_{\{i,j\}} S_i S_j - \frac{1}{J_b}\sum_i H(t) S_i, \qquad (1)$$

where the sum in the first term runs over pairs of nearest-neighbor spins that are in the surface layer $L = 1$. In the second

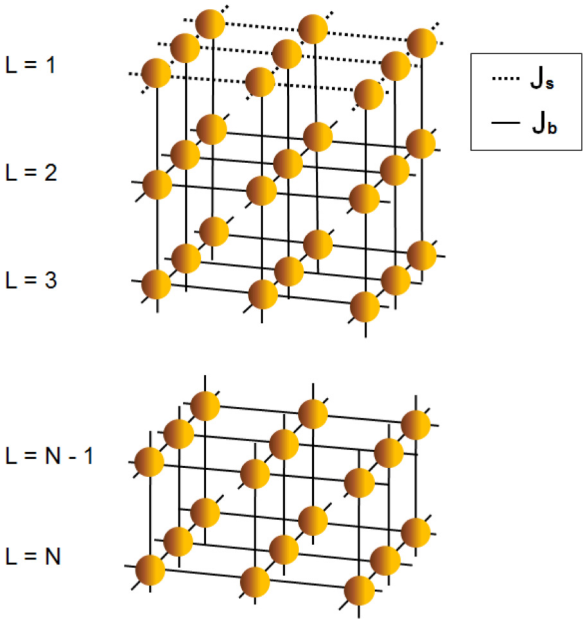

FIG. 1. (Color online) Schematic representation of the simple cubic lattice with the (100) surface orientation utilized in this study. Each atom in layer $L = 1$ (surface) has four in-plane nearest neighbors and interacts with them via an exchange coupling strength J_s, which is represented by dashed lines. Additionally, it has one other nearest neighbor in $L = 2$, to which it is coupled via exchange coupling strength J_b, represented with solid lines. For $L > 1$, each atom interacts with its six nearest neighbors through J_b, of which four are in-plane neighbors in L, one is in the layer above ($L - 1$), and one is in the layer below ($L + 1$).

term, the sum with curly brackets is applied to nearest-neighbor spins, of which at least one is not in the surface layer. The exchange coupling strengths J_s and J_b are given in units of energy and the spins S_i are dimensionless and restricted to values ± 1 for the sake of simplicity. The last term in (1) is the Zeeman energy summed over all the spins, assuming that surface and bulk moments have equal size regardless of the exchange coupling strength in between them. The magnetic field $H(t)$ is the sum of a periodic oscillating field and a continuous bias field H_b:

$$H(t) = H_0 \cos\left(\frac{2\pi}{P}\, t\right) + H_b, \tag{2}$$

with the magnetic fields H_0 and H_b given in units of energy. Here P is the period of the oscillating field. In the following we will represent all magnetic fields normalized to J_b by lowercase letters, i.e., $h(t) = H(t)/J_b$, $h_0 = H_0/J_b$, and $h_b = H_b/J_b$.

In the MFA, the complexity of the Hamiltonian (1) is simplified by the suppression of fluctuations, which allows for a representation of the Hamiltonian as a sum of products of spins S_i and local effective fields $h_L^{\text{eff}}(t)$ that depend on the layer L, in which each of the spins is located. This can be done because the MFA does not require translational invariance and has actually been used to solve the equilibrium Ising model for layered systems [29,31]. Within the MFA, we have

$$\tilde{\mathcal{H}}_{\text{MFA}} = \sum_{i(L)} h_L^{\text{eff}}(t) S_i. \tag{3}$$

The effective field $h_L^{\text{eff}}(t)$ is the sum of the external field $h(t)$ and the mean field arising from the magnetization of the neighboring atoms and is given as

$$h_1^{\text{eff}}(t) = h(t) + \frac{1}{6J_b}[4J_s m_1(t) + J_b m_2(t)], \tag{4a}$$

$$h_{L\neq 1,N}^{\text{eff}}(t) = h(t) + \frac{1}{6J_b}[4J_b m_L(t) + J_b m_{L-1}(t) + J_b m_{L+1}(t)], \tag{4b}$$

$$h_N^{\text{eff}}(t) = h(t) + m_N(t), \tag{4c}$$

with m_L being the spin expectation value of layer L. For the surface layer $L = 1$, the coupling strength towards the four in-plane nearest neighbors is J_s and the coupling strength to the neighbor in $L = 2$ is J_b. The atoms in the rest of the layers are coupled to their six nearest neighbors (four in plane, one above, and one below) via the exchange coupling strength J_b. The interactions have been normalized to 6 J_b, i.e., the interaction of an atom in the bulk. It should be noted that for layer N in Eq. (4c), the spins are coupled as if the system were a pure bulk system. Thus, layer N represents a bulk layer and not the central layer of a finite film system. If N is sufficiently large, this specific choice for layer N does not affect the fundamental behavior of the system. Instead, the advantage is that coupling this layer to itself provides a clear reference point for the inferred bulk behavior in terms of the critical period P_c, which is independent of N.

Assuming that the system follows stochastic Glauber dynamics, the time-dependent magnetization of every layer $m_L(t)$ is obtained by solving for each layer the dynamic equation that describes the approach to equilibrium [1]

$$\tau \frac{dm_L}{dt} = -m_L + \tanh\left(\frac{1}{T} h_L^{\text{eff}}\right). \tag{5}$$

Here τ is the relaxation time of the spin system and T is the temperature of the system normalized to its critical temperature T_c. The magnetization of each layer depends on the magnetization of the neighboring layers through the h_L^{eff} term, leading to a system of N coupled differential equations. Once $m_L(t)$ is known, one can compute the dynamic order parameter for each layer

$$Q_L = \frac{1}{P}\int_0^P m_L(t)dt \tag{6}$$

and the layer-resolved susceptibility [45]

$$\chi_L = \frac{dQ_L}{dh_b}. \tag{7}$$

The steady-state solutions of (5) have been determined numerically by discretizing one period of the oscillating field into K time steps. This discretization is performed by replacing $\frac{2\pi}{P}t$ with $2\pi\frac{k}{K}$, where k is an integer that ranges from 1 to K. Thus, the time-dependent functions $m_L(t)$ and $h_L^{\text{eff}}(t)$ can be rewritten as functions of the discrete variable k, i.e., $m_L(k)$ and $h_L^{\text{eff}}(k)$. The evaluation of Eq. (5) by means of finite differences leads to the system of $N \times K$ equations

$$m_L(k) = F(m_L(k)) = \frac{(\tau K/P)m_L(k-1) + \tanh\{(1/T)[h_L^{\text{eff}}(k)]\}}{1 + \tau K/P}, \tag{8}$$

which is solved self-consistently in an iterative process

$$m_L^{i+1}(k) = F\left(m_L^i(k)\right), \tag{9}$$

where i is the iteration index. The process is initialized with

$$m_L^{i=1}(k) = 0.15 + 0.4\cos\left(2\pi\frac{k}{K}\right) \tag{10}$$

if not stated otherwise and continued until $m_L^{i+1}(k) - m_L^i(k) < \epsilon$ is satisfied for all layers L and all time steps k, under the assumption that if this condition is fulfilled, self-consistency has been achieved. The cutoff criterion ϵ is chosen to be 10^{-11}. The number of k points utilized in our calculations is $K = 200$ and the number of layers is $N = 50$. We have tested that these values ensure convergence and that they are sufficient for the purposes of our study. We perform our calculations at a fixed temperature of $T = 0.8$, thus restricting ourselves to the parameter range in which only second-order dynamic phase transitions occur. By doing so we avoid first-order dynamic phase transitions that may be an artifact of the MFA itself [46]. We vary the period of the oscillating field P, its amplitude h_0, and the surface exchange coupling strength J_s. The study is performed at bias field $h_b = 0$, for which the critical point occurs. In the following we will denote surface quantities (corresponding to $L = 1$) by the subscript (or superscript) s and all the bulk quantities ($L = N$) by b.

III. RESULTS AND DISCUSSION

A. Bulk-terminated surface ($J_s = J_b$)

In order to investigate the behavior of surfaces at or near the DPT, we first analyze the $J_s = J_b$ case. With this value of J_s, the surface would not order by itself at the bulk critical period. This is the case because, even if the exchange coupling among spins is the same for the surface and bulk, the missing neighbors at the surface reduce the effective coupling strength. Thus, the surface alone would have a transition at a lower P than the bulk. However, being coupled to the bulk, some order is induced at the surface via the dynamically ordered bulk and its own DPT at a period below the bulk critical value is absent. Thus, if there is a surface DPT, it will be bulk supported and taking place at $P_c^s = P_c^b \equiv P_c$. Correspondingly, the system would exhibit an ordinary transition. However, Tauscher and Pleimling have found that the DPT in this ordinary transition regime is actually absent at the surface [40]. Our calculations confirm that this indeed happens for low values of the amplitude of the oscillating field h_0.

In Fig. 2(a) the time-dependent magnetization curves of the surface and the bulk are plotted as a function of time for three different values of P for a field of $h_0 = 0.080$. In this low-field case the critical period is $P_c = 93.375\,85\tau$, meaning that the dynamics is quite slow. Both the bulk and surface magnetizations can reverse their sign when $P > P_c$ and they oscillate symmetrically around zero, giving rise to a vanishing dynamic order parameter, as can be seen for the $P = 2P_c$ and $1.2P_c$ curves in Fig. 2(a). As the period of the oscillating field is further decreased though, the bulk magnetization cannot be reversed and its period-averaged value differs from zero and a dynamically ordered phase is achieved. As observed in the bottom graph of Fig. 2(a), for $P = 0.8P_c$ there are two solutions for the bulk magnetization, oscillating around a value of Q_b that has the same magnitude but opposite sign. The surface has also two solutions with the same property, but in this case both curves are very similar to each other and oscillate almost symmetrically around zero. Thus, the induced Q_s at the surface is very small. This qualitative difference in between the bulk and surface behavior can be readily observed in Fig. 2(b). Upon approaching the bulk critical period from above, both Q_b and Q_s are zero, but at P_c the bulk shows a clear onset of the dynamic order parameter Q_b, whereas Q_s only increases very gradually. Additionally, the bulk susceptibility, shown in Fig. 2(c), has a very pronounced peak at P_c [47], which is consistent with the expected divergence of the susceptibility at the critical point. However, the surface does not show any peak and therefore it is not undergoing a phase transition. The behavior reported by Tauscher and Pleimling [40] is thus confirmed in this particular case in that the surface does not undergo a bulk-supported DPT at P_c for the specific J_s and h_0 values chosen here.

The situation changes dramatically when the amplitude of the oscillating field is increased. For $h_0 = 0.375$, the bulk critical period is reduced ($P_c = 7.140\,62\tau$) and a behavior that resembles the equilibrium case is observed. Specifically, we find that the surface starts to order for $P < P_c$ with Q_s following a linear behavior as a function of P that is mimicking the surface magnetization vs temperature behavior of the equilibrium MFA case [30]. Figure 2(d) furthermore shows that the surface is exhibiting considerably larger Q_s values for $P < P_c$ in the $h_0 = 0.375$ case if compared to the $h_0 = 0.080$ case. Moreover, one can see in Fig. 2(e) that the surface susceptibility now shows a clear peak. Hence, the

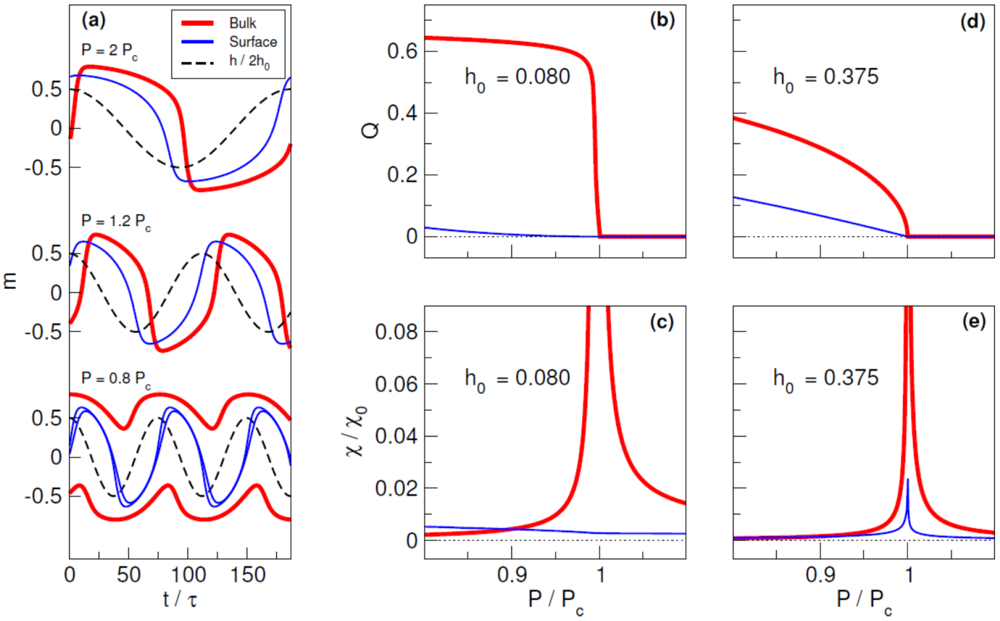

FIG. 2. (Color online) (a) Magnetization of the surface and bulk layers as a function of time (normalized by τ) for an oscillating field amplitude $h_0 = 0.080$ and for oscillating periods of $P = 2\,P_c$, $1.2P_c$, and $0.8P_c$ ($P_c = \ 93.375\,85\tau$). The magnetic field normalized to double its amplitude is represented by dashed (black) lines. The dynamic order parameter Q of the surface and bulk layers is shown as a function of the period P of the oscillating field normalized to P_c for (b) $h_0 = 0.080$ and (d) $h_0 = 0.375$. (c) and (e) Susceptibilities of the surface χ_s and bulk χ_b normalized to χ_0, as a function of P/P_c, corresponding to the order parameters in (b) and (d), respectively. All surface quantities are represented with thin (blue) solid lines and the bulk quantities with thick (red) solid lines. The surface coupling constant is $J_s = J_b$ in all cases.

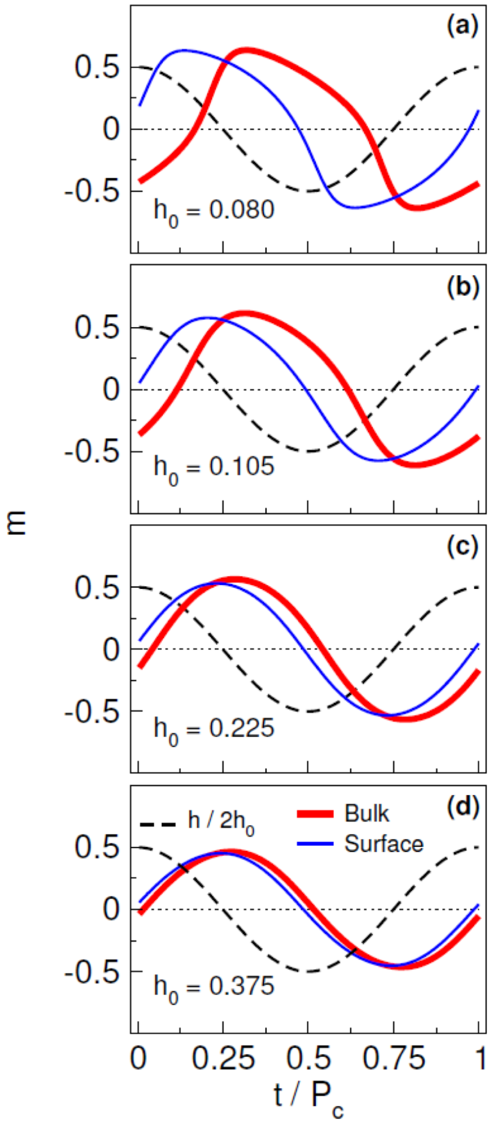

FIG. 3. (Color online) Magnetization m of the surface [thin (blue) solid line] and the bulk [thick (red) solid line] as a function of time t normalized to P_c, for different values of h_0. The period of the oscillating field in each case is the P_c value that corresponds to each respective amplitude h_0. The magnetic field normalized to double its amplitude is depicted as a dashed (black) line in each figure. A decreasing phase shift between surface and bulk magnetizations can be observed upon changing from (a) to (d), which corresponds to successively increasing h_0 values as indicated in each figure. The surface coupling constant is $J_s = J_b$ in all cases.

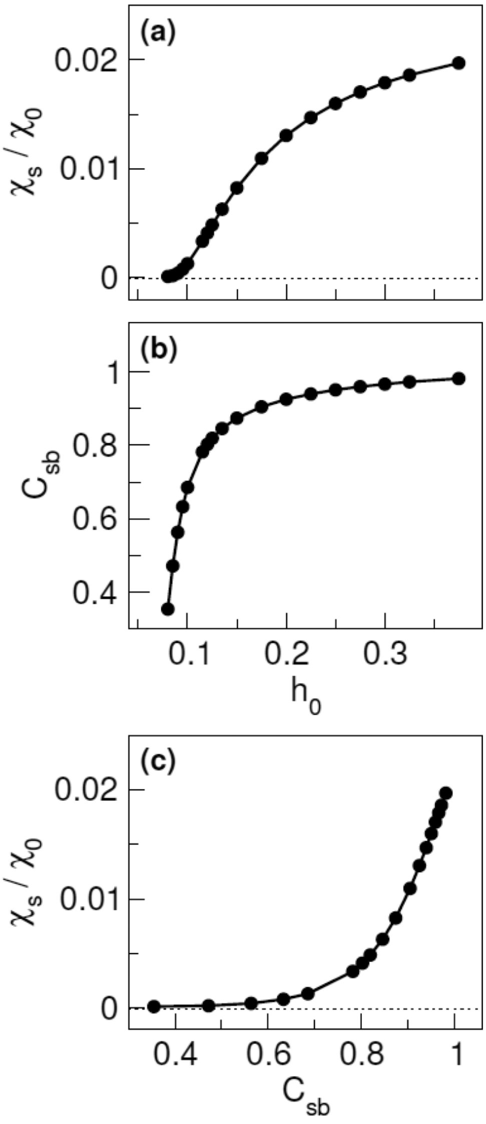

FIG. 4. (a) Surface susceptibility χ_s at P_c normalized by the bulk susceptibility at the same point, as a function of h_0 [47]. (b) Time correlation C_{sb} between the surface and the bulk magnetizations at P_c as defined in Eq. (11), as a function of h_0. (c) Relationship between the surface susceptibility peak at P_c and C_{sb}. In all figures, closed circles represent numerical calculations with the solid line being a guide to the eye. The surface coupling constant is $J_s = J_b$ in all cases.

surface is undergoing a DPT. These two cases illustrate that the bulk-supported DPT at the surface does not have a universal behavior, but instead depends strongly on h_0.

To understand the underlying reasons behind this nonuniversal behavior, we have analyzed the time-dependent magnetizations of bulk and surface at the bulk critical point P_c for different values of h_0. Four such time sequences are depicted in Fig. 3. For low h_0 (high P_c), the surface and bulk magnetizations show a substantial phase shift. Upon going from Fig. 3(a) to Fig. 3(d) by increasing h_0 (and thus decreasing P_c), the phase shift between surface and bulk magnetizations diminishes substantially and the two curves become more synchronous. This increasing synchronization permits the bulk, which is undergoing a DPT at P_c, to induce a surface DPT when the value of h_0 is large. In contrast, the low synchronization at low values of h_0 prevents this support of the surface transition by the bulk and that is the underlying reason why the surface does not show a DPT in Figs. 2(b) and 2(c). The h_0 influence on the surface DPT can be seen clearly in Fig. 4(a), where we find that the surface susceptibility χ_s at the bulk P_c increases monotonically with h_0.

For the purpose of quantifying the synchronization between surface and bulk magnetizations, we have calculated the time-correlation function

$$C_{sb} = \frac{\langle m_s m_b \rangle}{\sqrt{\langle m_s^2 \rangle \langle m_b^2 \rangle}}. \tag{11}$$

Here angular brackets represent the time average, numerically calculated as $\langle m_s m_b \rangle = \frac{1}{K}\sum_{k=1}^{K} m_s(k) m_b(k)$ and $\langle m_L^2 \rangle = \frac{1}{K}\sum_{k=1}^{K} [m_L(k)]^2$, where the layer L can be the surface s or the bulk b. Figure 4(b) shows that C_{sb} is a monotonically increasing function of h_0, which confirms the qualitative observation visible as apparent phase shifts in Fig. 3. It should be pointed out that this behavior is somewhat counterintuitive. Large h_0 values lead to fast critical dynamics, i.e., low P_c values, but nonetheless, it is in this very limit that the correlation between surface and bulk magnetization asymptotically approaches complete correlation $C_{sb} = 1$. On the other hand, complete correlation is also existent for the equilibrium case, where $h_0 = 0$. This is the reason why in the equilibrium case the surface always has a bulk-supported phase transition at the bulk T_c for $J_s = J_b$, because the surface and the bulk magnetizations are fully correlated in terms of their time-averaged behavior.

In Fig. 4(c) we have plotted the surface susceptibility at P_c as a function of C_{sb}. It can be observed that this relation has an onset behavior, with a threshold value of C_{sb}, above which the height of the surface susceptibility peak increases very steeply. Indeed, the correlation between surface and bulk magnetizations has to reach a certain value so that the bulk can effectively induce a surface DPT. If C_{sb} is not sufficiently high to trigger the surface DPT, the surface behaves as a nearly isolated system with respect to the bulk in the vicinity of P_c. Nevertheless, even in this case, the surface gets weakly and gradually polarized and thus does not undergo its own DPT at a P value smaller than P_c.

Consistent with these observations, the value of h_0 is also affecting the critical behavior of the surface layer in a most substantial fashion. When approaching the critical period, the dynamic order parameter follows a power-law behavior

$$Q_s = A_s (P_c - P)^{\beta_s}, \tag{12}$$

which is reminiscent of the $m_s \propto (T_c - T)^{\beta_s^{\mathrm{eq}}}$ law of the equilibrium case. The same power-law behavior (12) applies to the bulk, with the corresponding Q_b, A_b, and β_b parameters. Within the MFA, the critical exponent for the surface in the equilibrium Ising model is known to be $\beta_s^{\mathrm{eq}} = 1$ [30]. For the dynamic case, we have performed least-squares fits of our simulation results using Eq. (12) to obtain the value of β_s and we have found that it deviates from β_s^{eq}, a fact that had also been observed already in [36]. We observe that the deviation is substantial for low values of h_0, as can be seen in Fig. 5(a). However, β_s approaches the equilibrium value at high h_0. Additionally, in Fig. 5(b) we have plotted the ratio between the proportionality constants for Q_s and Q_b in the critical regime, i.e., A_s/A_b. The value of this ratio collapses for small h_0, which corroborates that the ordering of the surface is suppressed when the time correlation between surface and bulk magnetizations is small, in complete agreement with the results and discussion of Fig. 4.

Furthermore, it should be mentioned that the surface layer is not the only layer in which the DPT can be suppressed at low h_0. The layers immediately beneath the surface are affected as well, which can be demonstrated by a layer-resolved analysis. In Fig. 6 the susceptibility of the first 25 layers is plotted as a function of the oscillation period P and the layer index L. For $h_0 = 0.080$ [Fig. 6(a)] the susceptibility peak coming from the bulk DPT and appearing as a dark horizontal line here does not extend all the way to the surface and there are several dead magnetic layers from $L = 1$ to about $L = 6$ that do not show a susceptibility peak. For the case of $h_0 = 0.375$ in Fig. 6(b), however, all the layers show a clear susceptibility peak, even if its amplitude is reduced close to the surface. Thus, all layers participate in the DPT in this case.

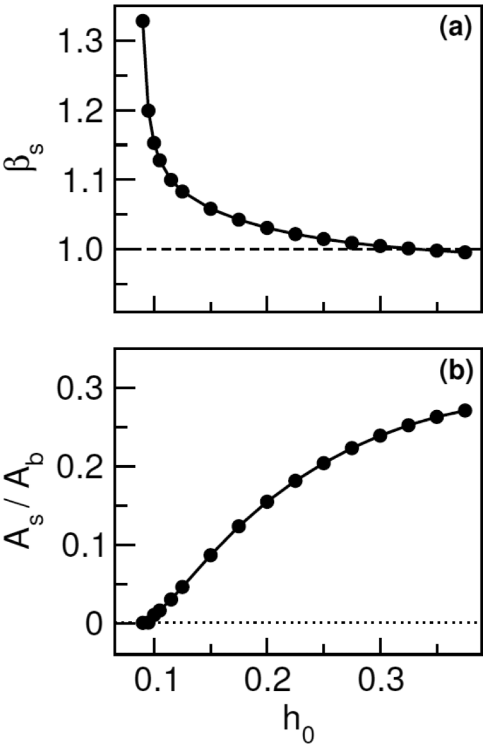

FIG. 5. (a) Critical exponent β_s as a function of h_0, obtained by fitting the computed data of Q_s with Eq. (12). The dashed line represents the equilibrium surface critical exponent in the MFA $\beta_s^{\mathrm{eq}} = 1$. (b) Ratio A_s/A_b between the prefactors of Eq. (12) as a function of h_0. In both cases, closed circles represent the numerical calculations and the solid line is a guide to the eye. The surface coupling constant is $J_s = J_b$ in all cases.

B. Modified surface exchange coupling ($J_s \neq J_b$)

In the second part of this work, we vary the value of J_s to be different from J_b. As a reference point, we pick the so-called special point [30,32,40], i.e., the J_s value, at which the surface orders at the same critical period as the bulk by itself without the need of being driven by the bulk. This condition is fulfilled for a simple cubic lattice with (100) surface orientation when $J_s = 1.25 J_b$ within the MFA. For $J_s = 1.25 J_b$ the dynamic magnetic state of the layered system is depth independent and it behaves as a pure bulk system without surfaces. Varying J_s will now allow for the study of the surface phase diagram as a function of P and J_s for different values of h_0.

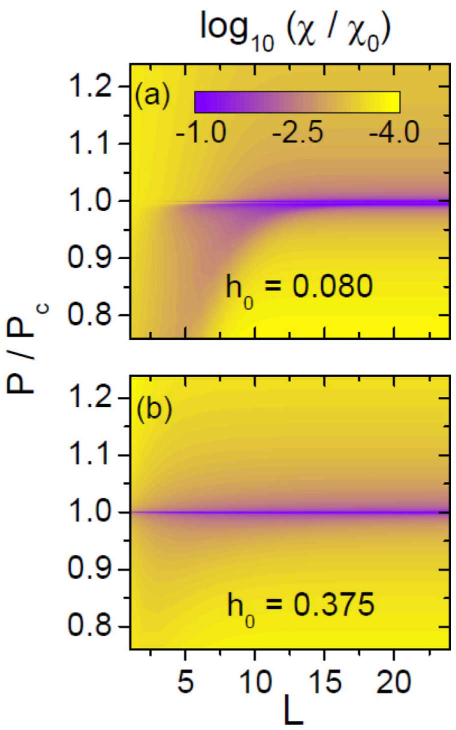

FIG. 6. (Color online) Normalized susceptibility χ/χ_0 maps as a function of the normalized period P/P_c and the layer index L, using a logarithmic (base 10) scale for χ/χ_0. The darkest regions represent high values of the susceptibility, i.e., peaks, and the light color corresponds to low values of the susceptibility. (a) The amplitude of the oscillating field is $h_0 = 0.080$ and the peak that comes from the bulk DPT does not extend to the topmost layers. (b) The amplitude of the oscillating field is $h_0 = 0.375$ and the peak extends all the way to the surface layer $L = 1$. The surface coupling constant is $J_s = J_b$ in both cases.

We shall first discuss the regime above the special point, i.e., when $J_s > 1.25J_b$. In this regime, the surface exchange coupling strength is large enough to produce a surface DPT that is separated from the bulk DPT, with $P_c^s > P_c^b \equiv P_c$. For such systems, the bulk DPT is still present at P_c and essentially unaffected by the surface DPT. Figures 7(a) and 7(b) show the surface susceptibility peaks for different J_s values as a function of P for $h_0 = 0.080$ and 0.375, respectively. The surface shows a clear susceptibility peak in all cases, verifying the existence of a DPT at the surface for J_s values above the special point, regardless of the value of h_0. The specific period value at which the surface DPT takes place varies with J_s, with larger J_s values leading to larger P_c^s. This fundamental behavior of the surface for $J_s > 1.25J_b$ does not vary with h_0 and it is qualitatively the same as in the equilibrium case, for which a surface phase transition is observed above T_c for sufficiently high J_s. There is only a quantitative difference for the different h_0 values that can be observed by directly comparing Figs. 7(a) and 7(b). The increase of P_c^s with J_s that we find in our calculations is steeper for low h_0. Indeed, in Fig. 7(a) ($h_0 = 0.080$) the surface susceptibility peaks for different values of J_s are more separated along the P axis than in Fig. 7(b). However, the key observation for $J_s > 1.25J_b$ is that the surface DPT always exists and is separated from the bulk DPT, just as in the equilibrium case. This observation is entirely consistent with the nonuniversal behavior we discussed for $J_s = J_b$. In that case, the presence or absence of a surface DPT was related to the synchronization of the bulk and surface magnetization behavior, as both have to undergo a single phase transition jointly. For the $J_s > 1.25J_b$ case, however, two separate phase transitions exist for the surface and the bulk, so synchronization in between the bulk and surface and correspondingly h_0 is not fundamentally relevant.

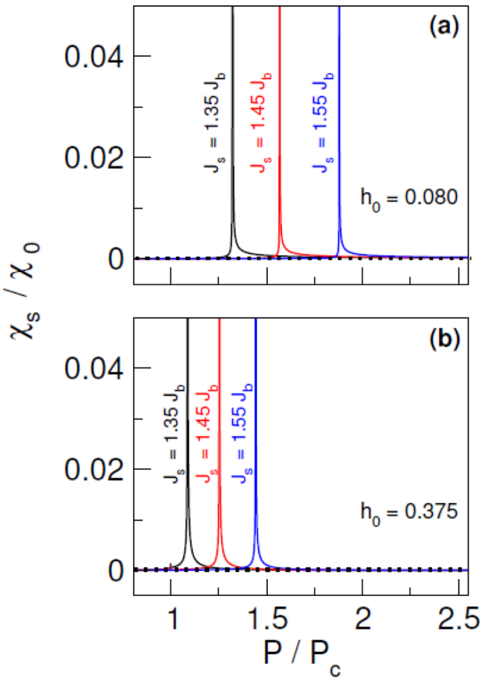

FIG. 7. (Color online) Normalized surface susceptibility χ_s/χ_0 as a function of the normalized period P/P_c for different J_s values above the special point. The J_s values, to which each curve corresponds, are given in the figure. They are, from left to right, $J_s = 1.35J_b$, $1.45J_b$, and $1.55J_b$. (a) The $h_0 = 0.080$ case and (b) the $h_0 = 0.375$ case.

It should also be mentioned that the surface DPT extends to several subsurface layers. This is visible in Figs. 8(a) and 8(b). Here the susceptibility of the first 25 layers is plotted as a function of P and the layer index L. The dark horizontal line at $P/P_c = 1$ corresponds to the DPT of the bulk and the secondary dark horizontal line at $P/P_c > 1$ corresponds to the susceptibility peak of the surface DPT. This secondary line is most pronounced for the topmost layers. The surface DPT weakens as one moves away from the surface and eventually disappears. The penetration of the surface DPT can be described accurately by an exponential decay as a function of L,

$$\chi_L = Be^{-L/\lambda} + c, \tag{13}$$

where λ is the penetration depth, c is the asymptotic bulk susceptibility at P_c^s, and B is a multiplicative constant. This is the same behavior as the one that is observed for the surface phase transition in thermodynamic equilibrium, namely, that the susceptibility related to the localized surface

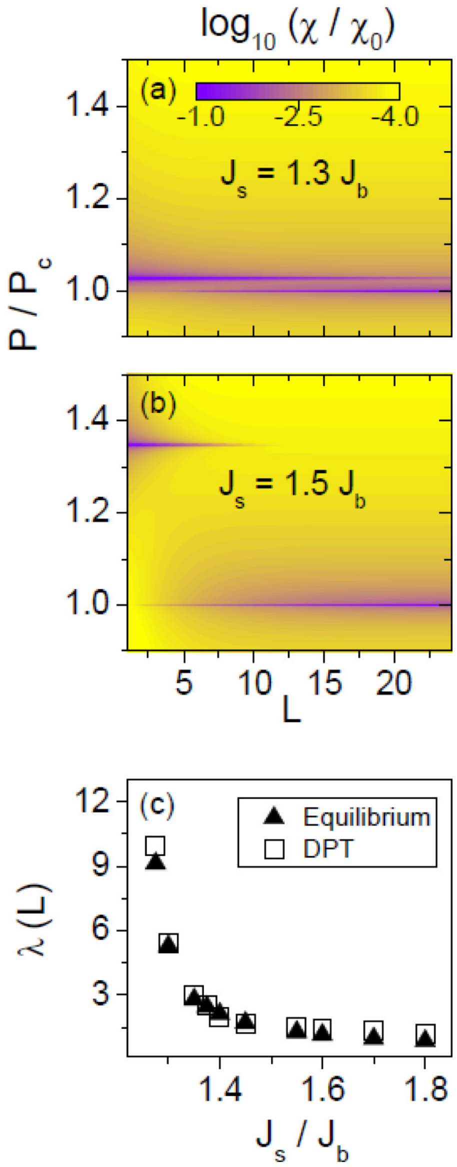

FIG. 8. (Color online) (a) and (b) Normalized susceptibility χ/χ_0 maps as a function of the normalized period P/P_c and the layer index L, using a logarithmic (base 10) scale for χ/χ_0, for $h_0 = 0.375$ and (a) $J_s = 1.3J_b$ and (b) $J_s = 1.5J_b$. Two peaks are observed: one occurring at P_c^s, with $P/P_c > 1$, corresponds to the surface transition and the other one at $P/P_c = 1$ is the bulk transition. In (a) the surface transition penetrates more deeply into the bulk than in (b). (c) Penetration depth λ of the surface transition in units of L, as a function of J_s. Here λ has been obtained by fitting Eq. (13) to our numerical susceptibility χ vs L data. For the DPT case (shown as open squares) all fits were done at the surface critical period P_c^s. In the equilibrium case (shown as closed triangles), the fits of χ vs L were performed at the surface critical temperature T_c^s.

phase transition falls off exponentially as a function of the depth [30]. As one can see from Fig. 8, λ depends strongly on J_s. If J_s is close to the special point, as in Fig. 8(a) with $J_s = 1.3J_b$, P_c^s will only be slightly higher than P_c and the surface transition can penetrate very efficiently into the subsurface region. If J_s is increased further, as in Fig. 8(b) with $J_s = 1.5J_b$, the bulk and surface transitions will separate significantly in P and the latter will exhibit a stronger surface localization, only affecting a few of the topmost layers. We have performed least-squares fits of Eq. (13) to our numerical calculations to obtain λ for different values of J_s. The results are plotted in Fig. 8(c) as open squares. The strong dependence of the penetration depth on J_s is very visible from these data. By analyzing and comparing data for the equilibrium Ising model, we found that equilibrium and dynamic nonequilibrium surface transitions behave in the exact same way. The decrease of λ vs J_s for the equilibrium surface phase transition, depicted as closed triangles in Fig. 8(c), exhibits the same behavior that we observe for the DPT at surfaces.

So overall, the equilibrium and the nonequilibrium phase diagrams and the associated physical behavior are fundamentally identical in the high J_s regime, in agreement with the observations in [40]. This is true regardless of the specific value of h_0.

In the following we will analyze the $J_s < 1.25J_b$ case. In this regime, the surface order at the bulk P_c has to be induced by the bulk. As we have already seen for the $J_s = J_b$ case, this behavior is strongly h_0 dependent and for low h_0 values, the surface and the layers close to it do not undergo a DPT. Figure 9 shows the susceptibility for the first 15 layers as a function of the period P and the layer index L for low and high values of h_0 and for different values of J_s. In the low-field case with $h_0 = 0.080$, shown on the left-hand side in Fig. 9, the topmost layers do not participate in the DPT in Figs. 9(a)–9(c), which correspond to values of $J_s = 0.8J_b$, $0.9J_b$, and $1.1J_b$, respectively. This is clearly evident because the dark horizontal line corresponding to the bulk DPT does not extend all the way to the surface or the surface near the layers. We observe that the susceptibility of layers 1–6 does not show any substantial peak at $P = P_c$ until the special point with $J_s = 1.25J_b$ is reached, as is shown in Fig. 9(d). So we can conclude that in the low h_0 case there is no bulk-supported surface DPT for $J_s < 1.25J_b$. Conversely, for the $h_0 = 0.375$ calculations shown on the right-hand side of Fig. 9, the surface and the layers close to it show a clear susceptibility peak for values of J_s as low as $0.8J_b$. Increasing J_s towards the special point as observed in Fig. 9(h) makes this peak slightly more pronounced, but does not fundamentally alter the physics. The bulk-supported DPT occurs at high-h_0 amplitudes, even for J_s values that are reduced with respect to the bulk-terminated case $J_s = J_b$.

For practical purposes, we define here a criterion to determine whether the surface DPT is existent and observable. Specifically, we define that the surface is undergoing a bulk-supported DPT at the bulk P_c if the ratio between the surface and the bulk susceptibility χ_s/χ_0 at this point is higher than 0.01 [47]. The fundamental aspects of the corresponding classification will not depend on the specific numerical value chosen, which is somewhat artificial and chosen for convenience and detectability under experimental or numerical noise conditions. With this definition, we can now study the surface phase diagram as a function of J_s and P. Several such diagrams are plotted in Fig. 10 for different values of h_0. For each h_0, the bulk transition (dashed line) has the same P_c, independent from the value of J_s, because the systems under consideration here are thick enough so that

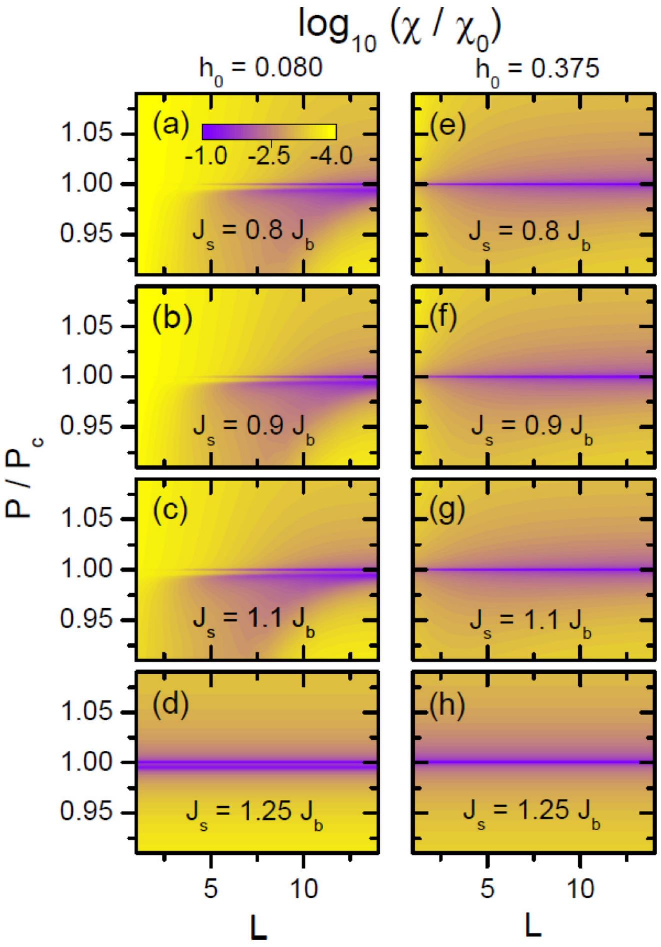

FIG. 9. (Color online) Normalized susceptibility χ/χ_0 maps as a function of the normalized period P/P_c and the layer index L, using a logarithmic (base 10) scale for χ/χ_0, for (a)–(d) $h_0 = 0.080$ and (e)–(h) $h_0 = 0.375$. The respective values of J_s are shown in each panel.

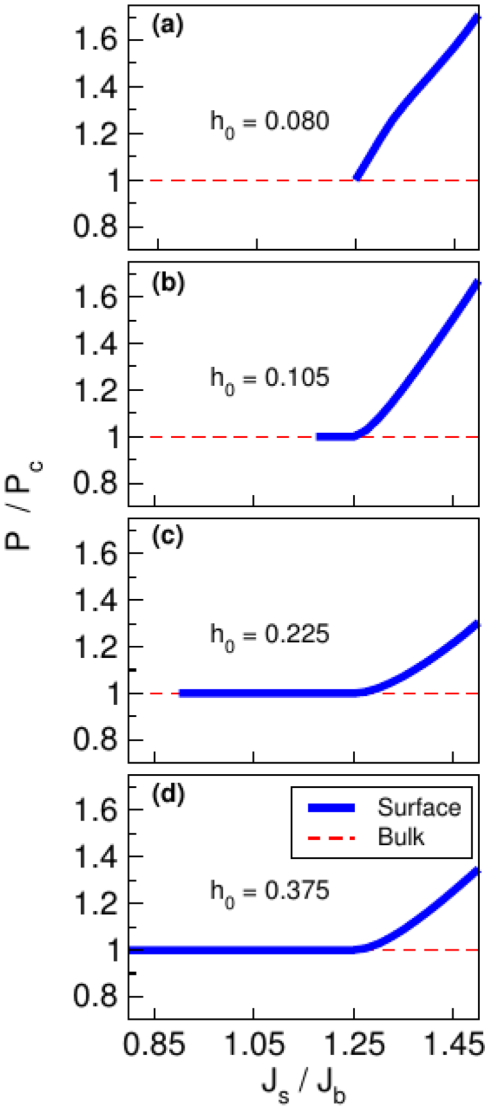

FIG. 10. (Color online) The $J_s - P$ surface phase diagrams for different amplitudes of the oscillating field h_0. The lines represent the boundaries between the phases and are determined from the respective positions of the susceptibility peaks. The surface phase boundaries are depicted as solid (blue) lines and the bulk phase boundaries as dashed (red) lines. The vertical axis corresponds to the period normalized to the bulk critical period in each case and the horizontal axis to the ratio between surface and bulk coupling strengths.

bulk transitions are not affected by surface properties [48]. The surface DPT behavior, shown as a solid line in each case, however, is not so simple. In Figs. 10(a)–10(d) the isolated surface DPT, which occurs above the special point, i.e., $J_s > 1.25J_b$, is always present and P_c^s increases monotonically with J_s in each case. In Fig. 10(a), corresponding to an applied field of $h_0 = 0.080$, we find the surface only to have a DPT at or above the special point. Below it, the correlation between the surface and bulk magnetizations is too low for the bulk to drive a surface DPT. However, as h_0 and consequently C_{sb} are increased, the bulk-supported surface DPT starts to be observable even for values of $J_s < 1.25J_b$, which can be seen in Figs. 10(b)–10(d). This alteration of the phase diagram happens because the dynamic surface magnetization becomes ever more correlated to the dynamic bulk magnetization. The higher h_0 is, the further the surface DPT extends towards the low J_s range. In particular, one can see in Fig. 10(d) that for $h_0 = 0.375$ the surface DPT is even present for values of J_s that are substantially lower than the $J_s = J_b$ bulk-terminated case.

In order to confirm that the physical mechanism that triggers the bulk-supported surface DPT is indeed the time correlation between the surface and bulk magnetization at P_c, we analyzed the height of the surface susceptibility peak at the bulk P_c as a function of C_{sb} for three different values of J_s below the special point and for several values of h_0 each. Indeed, we find that C_{sb} varies not only with h_0, but also with J_s. For each of our simulated J_s and h_0 pairs, we have computed χ_s and C_{sb}. Figure 11 shows χ_s as a function of C_{sb}, using different symbols for the different selected J_s values. This plot shows that regardless of J_s, all the data not only show an onset behavior, but are also fairly well described by the same universal curve. This corroborates that C_{sb} is the key physical quantity that determines if a system with surfaces exhibits a bulk-supported surface DPT.

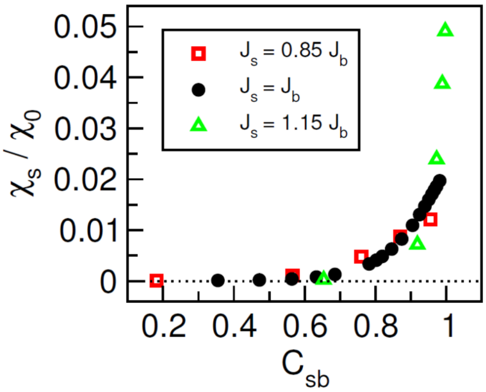

FIG. 11. (Color online) Normalized surface susceptibility at $P/P_c = 1$ as a function of the time correlation C_{sb} between surface and bulk magnetization. Values have been computed for different values of h_0 and J_s ($<1.25J_b$). Circles (black) represent values calculated for $J_s = J_b$, squares (red) correspond to $J_s = 0.85J_b$, and triangles (green) to $J_s = 1.15\ J_b$.

It should also be mentioned that the values of h_0 for which we detect a suppression of the surface DPT at the bulk P_c are lower than the corresponding h_0 values found by Tauscher and Pleimling [40]. This discrepancy can be ascribed to the fact that mean-field calculations generally do not give the same numerical values as MCSs for quantities such as critical temperatures or critical exponents. However, mean-field calculations frequently predict phase diagrams that are qualitatively consistent with those obtained by MCSs or other methods. Thus, we consider it likely that sufficiently high amplitudes of the oscillating field would allow for the observation of a bulk-driven surface DPT also by means of MCSs.

IV. CONCLUSION

We have performed a detailed study of the DPT in systems with surfaces, varying the surface exchange coupling strength J_s, the period P of the oscillating field, and its amplitude h_0. Our mean-field approximation approach has enabled us to explore a wide range of the parameter space, which has allowed us to identify the importance of h_0.

In accordance with previous studies, we found that for sufficiently high values of J_s, surfaces undergo a DPT separately from the bulk in the same way the equilibrium Ising model shows surface-localized thermodynamic phase transitions. Additionally, we observed that for low J_s values, for which the surface cannot order by itself at the bulk P_c, the surface DPT can be completely suppressed in agreement with the results reported by Tauscher and Pleimling [40]. However, our study shows that this is not a universal behavior. Instead, surfaces undergo a DPT at the bulk P_c for sufficiently strong h_0. The presence or absence of this bulk-supported surface DPT can be explained by the time correlation between the surface and the bulk magnetizations at the bulk critical point. The bulk is critical at P_c and when the surface and the bulk magnetizations are almost synchronous at this point, the surface is effectively coupled to the bulk and thus undergoes a DPT at this point as well. However, when the time correlation is below a threshold value, the bulk cannot support the surface DPT and no DPT at the surface occurs. Our calculation results show that the time correlation C_{sb} is the key quantity that determines the system's behavior, regardless of the value of J_s, assuming that it is below the so-called special point.

We hope this work stimulates further studies on the role of the amplitude of the applied oscillatory field onto the bulk and surface DPT, as it is the dynamic input variable that has no analog in the thermodynamic case. In addition, our calculations also suggest that the DPT can be suppressed in the topmost 5–6 atomic layers, which comprise a film of 1–2 nm thickness. Thus, it might very well be feasible to detect this anomalous and nonuniversal surface behavior experimentally with a technique that has sufficient selectivity and sensitivity, such as magneto-optical Kerr-effect-based magnetometry [49].

ACKNOWLEDGMENTS

We acknowledge funding from the Basque Government under Program No. PI2012-47 and the Spanish Ministry of Economy and Competitiveness under Project No. MAT2012-36844.

---

[1] T. Tomé and M. J. de Oliveira, Phys. Rev. A **41**, 4251 (1990).
[2] M. Rao, H. R. Krishnamurthy, and R. Pandit, Phys. Rev. B **42**, 856 (1990).
[3] M. Rao, H. R. Krishnamurthy, and R. Pandit, J. Appl. Phys. **67**, 5451 (1990).
[4] W. S. Lo and R. A. Pelcovits, Phys. Rev. A **42**, 7471 (1990).
[5] S. Sengupta, Y. Marathe, and S. Puri, Phys Rev. B **45**, 7828 (1992).
[6] Y. L. He and G. C. Wang, Phys. Rev. Lett. **70**, 2336 (1993).
[7] Q. Jiang, H. N. Yang, and G. C. Wang, Phys. Rev. B **52**, 14911 (1995).
[8] B. K. Chakrabarti and M. Acharyya, Rev. Mod. Phys. **71**, 847 (1999).
[9] M. Acharyya, Int. J. Mod. Phys. C **16**, 1631 (2005).
[10] M. Acharyya and B. K. Chakrabarti, Phys. Rev. B **52**, 6550 (1995).
[11] M. Acharyya, Phys. Rev. E **56**, 1234 (1997).
[12] S. W. Sides, P. A. Rikvold, and M. A. Novotny, Phys. Rev. Lett. **81**, 834 (1998).
[13] M. Acharyya, Phys. Rev. E **59**, 218 (1999).
[14] G. Korniss, C. J. White, P. A. Rikvold, and M. A. Novotny, Phys. Rev. E **63**, 016120 (2000).
[15] G. Korniss, P. A. Rikvold, and M. A. Novotny, Phys. Rev. E **66**, 056127 (2002).
[16] D. T. Robb, P. A. Rikvold, A. Berger, and M. A. Novotny, Phys. Rev. E **76**, 021124 (2007).
[17] G. M. Buendía and P. A. Rikvold, Phys. Rev. E **78**, 051108 (2008).

[18] S. Akkaya Deviren and E. Albayrak, Phys. Rev. E **82**, 022104 (2010).
[19] Y. Yüksel, E. Vatansever, U. Akıncı, and H. Polat, Phys. Rev. E **85**, 051123 (2012).
[20] O. Idigoras, P. Vavassori, and A. Berger, Physica B **407**, 1377 (2012).
[21] M. Ertas, B. Deviren, and M. Keskin, Phys. Rev. E **86**, 051110 (2012).
[22] R. A. Gallardo, O. Idigoras, P. Landeros, and A. Berger, Phys. Rev. E **86**, 051101 (2012).
[23] H. Park and M. Pleimling, Phys. Rev. E **87**, 032145 (2013).
[24] D. T. Robb and A. Ostrander, Phys. Rev. E **89**, 022114 (2014).
[25] D. T. Robb, Y. H. Xu, O. Hellwig, J. McCord, A. Berger, M. A. Novotny, and P. A. Rikvold, Phys. Rev. B **78**, 134422 (2008).
[26] A. Berger, O. Idigoras, and P. Vavassori, Phys. Rev. Lett. **111**, 190602 (2013).
[27] K. Binder and P. C. Hohenberg, Phys. Rev. B **6**, 3461 (1972).
[28] D. L. Mills, Phys. Rev. B **3**, 3887 (1971).
[29] R. A. Weiner, Phys. Rev. B **8**, 4427 (1973).
[30] K. Binder and P. C. Hohenberg, Phys. Rev. B **9**, 2194 (1974).
[31] F. Aguilera-Granja and J. L. Morán-López, Phys. Rev. B **31**, 7146 (1985).
[32] D. P. Landau and K. Binder, Phys. Rev. B **41**, 4633 (1990).
[33] T. Kaneyoshi, J. Phys.: Condens. Matter **3**, 4497 (1991).
[34] H. W. Diehl, Int. J. Mod. Phys. B **11**, 3503 (1997).
[35] M. Pleimling, J. Phys. A: Math. Gen. **37**, R79 (2004).
[36] H. Park and M. Pleimling, Phys. Rev. Lett. **109**, 175703 (2012).
[37] H. Park and M. Pleimling, Phys. Rev. Lett. **110**, 239903(E) (2013).
[38] Y. Yüksel, E. Vatansever, and H. Polat, J. Phys.: Condens. Matter **24**, 436004 (2012).
[39] M. Boughrara, M. Kerouad, and A. Zaim, J. Magn. Magn. Mater. **331**, 37 (2013).
[40] K. Tauscher and M. Pleimling, Phys. Rev. E **89**, 022121 (2014).
[41] B.O Aktas, U. Akıncı, and H. Polat, Thin Solid Films **562**, 680 (2014).
[42] B. O. Aktas, U. Akıncı, and H. Polat, Phys. Rev. E **90**, 012129 (2014).
[43] Y. Yüksel, Phys. Rev. E **91**, 032149 (2015).
[44] We have verified that the choice of the lattice type does not alter the conclusions drawn from our simulation results. We find fcc, bcc, and hcp lattices all to show the same qualitative behavior described in the text.
[45] The susceptibility is computed numerically as $\frac{Q(h_b=\delta)-Q(h_b=0)}{\delta}$, for which we utilize $\delta = 10^{-7}$.
[46] G. Berkolaiko and M. Grinfeld, Phys. Rev. E **76**, 061110 (2007).
[47] Given the fact that the bulk susceptibility diverges at the DPT, a numerical comparison with this diverging quantity is not always meaningful, especially when plotting numerically calculated data. Thus, we use in our data analysis and visualization another, more practical reference point. Specifically, we use the bulk susceptibility $\chi_b(P = 1.000\,01 P_c)$ for every value of h_0, to which we then refer to as χ_0 in each case.
[48] In all the calculation results shown here, the bulk layer $L = N$ is coupled to itself as described by Eq. (4). So, with this constraint, the bulk P_c would always be independent of J_s, no matter how thick the system is, i.e., regardless of the value of N. However, we have verified in a different series of calculations, in which layer N is a true central layer of a finite-thickness film (total thickness $2N - 1$), that Fig. 10 and all other relevant results look identical on the scale shown in each figure.
[49] A. Berger, S. Knappmann, and H. P. Oepen, J. Appl. Phys. **75**, 5598 (1994); M. R. Pufall, C. Platt, and A. Berger, *ibid.* **85**, 4818 (1999).